

## Research Article

# Fabrication and Characterization of Alkyl-Functionalized CNFs/Cellulose Acetate Polymer Nanocomposites

Situma Stephen Mukhebi<sup>1,\*</sup> , Geoffrey Otieno<sup>1</sup> , Austin Ochieng Aluoch<sup>1</sup> ,  
Dickson Mubera Andala<sup>2</sup> , James Owour<sup>1</sup> 

<sup>1</sup>School of Chemistry and Material Science, Technical University of Kenya, Haile Selassie Avenue, Nairobi, Kenya

<sup>2</sup>Chemistry Department, Multimedia University of Kenya, Nairobi, Kenya

## Abstract

Carbon nanofibers (CNFs) are widely used to fabricate nanocomposites with enhanced properties. The emergent properties of the nanocomposites depend on the initial properties of the CNFs and how the fibers have been dispersed within the polymer matrix. This study looks at the fabrication of nanocomposites using dodecyl, butyl, and acetyl functionalized CNFs with cellulose acetate as the polymer matrix. The CNFs were prepared by electro-spinning, and functionalization was achieved using alkyl halides in the presence of lithium. Scanning Electron Microscopy (SEM) showed that the fibers were well embedded in the polymer matrix. Thermal Gravimetric Analysis (TGA) of the nanocomposite revealed a slight increase in the degradation temperatures of the nanocomposites as compared to the blank sample, the aggregate loss of weight of the samples was about 80%. Dynamic Mechanical Analysis (DMA) of the nanocomposites showed increased stiffness and modulus storage by an average of 450MPa for butyl and dodecyl-functionalized CNFs, however, the storage modulus values of the nanocomposites generally decreased with an increase in temperature. The glass transition temperature of the nanocomposites was higher than that of the reference sample by an average of +36 °C. Conductivity measurements of the nanocomposites showed no changes at lower frequencies of  $1 \times 10^2 - 4 \times 10^4$  Hz. However, the values started increasing and peaked at  $5 \times 10^7$  Hz. The conductivity measurements revealed that the nanocomposites exhibited higher conductivity peaks at specific frequencies compared to the reference sample, indicating an enhanced electrical property of the nanocomposite. The study successfully fabricated nanocomposites with enhanced mechanical, thermal, and dielectric properties using functionalized CNFs.

## Keywords

Carbon Nanofibers, Alkylation, Cellulose Acetate, Carbon Nanocomposites

## 1. Introduction

The use of carbon nanofibres (CNFs) to fabricate nanocomposites with improved physical, mechanical, and electrical properties is widely reported [1-4]. Carbon nanofibers have several applications that are hinged on the mode of prepara-

tion and various treatments that they can undergo, like heat treatments, and blended with additional elements to form useful nanocomposites.

The specific characteristics of CNF/polymer nanocompo-

\*Corresponding author: [Stephen.situma@nacosti.go.ke](mailto:Stephen.situma@nacosti.go.ke) (Situma Stephen Mukhebi)

Received: 31 August 2024; Accepted: 19 September 2024; Published: 29 September 2024



Copyright: © The Author(s), 2024. Published by Science Publishing Group. This is an **Open Access** article, distributed under the terms of the Creative Commons Attribution 4.0 License (<http://creativecommons.org/licenses/by/4.0/>), which permits unrestricted use, distribution and reproduction in any medium, provided the original work is properly cited.

sites greatly depend on how well the CNFs are dispersed within the polymer matrix. Enhancing the dispersion of CNFs can lead to substantial improvements in properties such as modulus and compressive strength. The applications of CNF/polymer nanocomposites include Catalysts, the polymer solution is doped with nanoparticles of transitional metals like Titanium, rhodium, and Palladium [5]. The nano biosensors have been employed in disease diagnosis due to their high sensitivity towards the target molecule, good adsorption, and electron transferability that enhance the identification and treatment of common diseases.

Electrospun nanofibers coated with silver nanoparticles are widely used in bacterial control, when chitosan polymeric hydrogels, an active wound-healing reagent is added to the nanoparticles, a wound dressing material that has both healing and antibacterial properties is produced [6]. Due to their excellent electrical conductivity and mechanical strength, nano biofibers have also been used in cardiac tissue engineering [7].

The specific characteristics of CNF/polymer nanocomposites greatly depend on the% composition of the CNFs and how well they are dispersed within the polymer matrix [20]. Enhancing the dispersion of CNFs can lead to substantial improvements in properties such as modulus and compressive strength, as observed in the modulus of CNF/ polypropylene nanocomposite increase of 50% and compressive strength by 100% following a 5% increase in dispersion of the nanofibres into the polymer [1]. Moreover, modifying carbon nanofibers physically and structurally before integrating them into nanocomposites has been shown to yield nanocomposites with enhanced properties. For instance, reinforcing Polymethyl methacrylate-based carbon nanofibers with substances like magnesium oxide can result in nanocomposites with improved mechanical and biocompatibility attributes. [8-10].

In a previous study, *N*-alkylated methacrylate, methyl, cyclohexyl, and isobonyl carbon nanofibers enhanced the glass transition temperature of resulting nanocomposites by 10-15°C and displayed higher resistance towards sunshine degradation by 16 months compared to the unfunctionalized ones [11]. As such, chemical and structural modifications of carbon nanofibers present promising opportunities for further enhancing the properties of nanocomposites.

This work reports the fabrication of nanocomposites using dodecyl, *n*-butyl, and acetyl functionalized carbon nanofibres and cellulose acetate as the polymer matrix and the resulting properties including, mechanical strength, thermal properties and conductivity. We also report on how these properties change when the % concentration of the functionalized CNF is increased from 0.2 wt % to 0.4 wt% of the nanocomposite.

## 2. Materials and Methods

All chemicals and solvents used in the research work were sourced from reputable supplies such as Sigma-Aldrich (U.S.A) and were of analar grade. The chemicals included

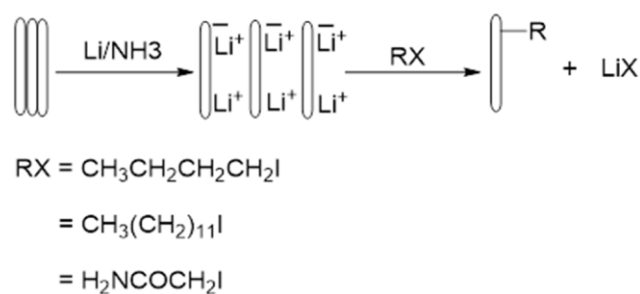
Poly methyl methacrylate, Lithium metal, Dimethylformamide, Dichloromethane, Ethanol, Chloroform, Iodobutane, IodoDodecane, Iodoacetamide, Ammonia solution, Hexane, methanol, Hydrochloric Acid, Cetyltrimethylammonium bromide, polyethylene glycol and 0.2 µm Polytetrafluoroethylene (PTFE) membrane filter.

### 2.1. Preparation of Carbon Nanofibres

The preparation of carbon nanofibers was carried out as previously described with slight modifications [12]. About 80 mg of analytical grade Polymethyl methyl acrylate (Sigma Aldrich) was dissolved in 10 ml of a dichloromethane/ dimethylformamide mixture in a ratio of 2:3 and stirred using a magnetic stirrer for 3 hours. The polymer solution was electrospun at 18 K v, 22 °C, and 45% humidity (BK precision 1901 32V/30a), and fibers were collected on aluminum foil placed 15 cm away from the tip of the pipette. The resulting nanofibers were allowed to dry at room temperature for 2 hrs and calcinated at 400 °C in an inert environment of nitrogen gas to yield black carbonized nanofibers.

### 2.2. Functionalization of Carbon Nanofibres

The functionalization of the carbon nanofibres was carried out by first putting the nanofibers into the oven-dried 100 ml three-neck round-bottom flask. Ammonia solution was then added to the condensed flask, to the mixture small pieces of lithium metal were added, the glass flask was slowly swirled till all the metal had reacted. The alkyl iodide was then added, and the reaction mixture was stirred overnight with the slow evaporation of NH<sub>3</sub>. The mixture was then cooled in an ice bath and some 100 ml of methanol was added slowly followed by 20 ml of water. After acidification (10% HCl), the nanofibers were extracted using hexane and washed several times with water [13, 19]. The hexane layer was filtered through a 0.2 µm PTFE membrane filter, washed with ethanol, and dried in a vacuum oven at a temperature of 80 °C overnight. The reaction mechanism for the functionalization of the CNF is shown in scheme 1 below.



**Scheme 1.** Functionalization of carbon nanofibers by alkylation [13].

### 2.3. Solubility Test of Cellulose Acetate Polymer in Selected Solvents

The cellulose acetate polymer was tested for uniform dispersion in acetone, chloroform, dichloromethane, hexane, and *N, N*-dimethylformamide by adding 20 mg of sample in the 100 ml of solvent at room temperature and sonicating for an hour then observed for one hour.

### 2.4. Preparation of 0.2% Alkyl Nanocomposites

A mixture of 0.02 g of alkyl functionalized carbon nanofiber (*n*-butyl, acetyl or dodecyl), 0.01 g of Cetyltrimethylammonium bromide, and 30 ml acetone were added to a dry 100 ml flask and ultrasonicated for 2 hours. In a different dry 100 ml flask, a mixture of 7.97 g of Cellulose acetate, 2.0 g of polyethylene glycol, and 50 ml of acetone was stirred to completely dissolve cellulose acetate. The two solutions were mixed, ultra-sonicated for 6 hrs, poured onto a flatbed, glass vessel, to allow solvent evaporation, then put in an oven at 40 °C overnight to form a thin film of alkyl nanocomposite.

### 2.5. Preparation of 0.4% Alkyl Nanocomposite

A mixture of 0.04 g of alkyl functionalized carbon nanofiber (*n*-butyl, acetyl or dodecyl), 0.02 g of Cetyltrimethylammonium bromide and 50 ml of acetone were added to a 100 ml dry flask and ultrasonicated for 2 hours. In a different dry 100 ml flask, a mixture of 7.97 g of Cellulose acetate, 2.0 g of polyethylene glycol and 50 ml of acetone was stirred to completely dissolve cellulose acetate. The two solutions were mixed, ultra-sonicated for 6 hrs, poured onto a flatbed, glass vessel, to allow solvent evaporation, then put in an oven at 40 °C overnight to form a thin film of alkyl nanocomposite.

## 3. Characterization of the Nanocomposites

### 3.1. Solubility of the Cellulose Acetate Polymer in Selected Solvents

The solubility of cellulose acetate polymer was tested with several solvents (Acetone, *N, N*-dimethylformamide, chloroform and *n*-hexane). It was found to be whole soluble in acetone and *N, N*-dimethylformamide but insoluble in chloroform and *n*-hexane. From this, Acetone and *N, N*-dimethylformamide in the ratio 1:1 was selected as the solvent system in preparation of carbon nanofiber/ Cellulose polymer nanocomposites.

### 3.2. Scanning Electron Microscopy (SEM) and Energy Dispersive Spectroscopy (EDS)

Scanning Electron Microscopy and Energy Dispersive

Spectroscopy (EDS) was done using a Zeiss EVO LS15 Scanning Electron Microscope, with accelerating voltage of 5 or 8 kV. Film samples were prepared by embedding and leaving them to dry overnight. A microtome was then used to cut a cross section of the sample and resin on one side resulting in a smooth surface of the sample. The sample was coated with gold to avoid melting and microscopy was conducted to determine its morphology.

### 3.3. Thermogravimetric Analysis (TGA)

A 20.0 mg of nanocomposite sample was subjected to Thermogravimetric Analysis and Derivative Thermogravimetric analysis under inert environment conditions using N<sub>2</sub> gas at a flow rate of 20 ml/min. Analysis temperature was increased from 30°C to 800°C at a rate of 10°C/min (TGAQ/DSCI machine).

### 3.4. Dynamic Mechanical Analysis

The mechanical properties of the nanocomposites were determined using the Mettler Toledo instrument DMA1 with Mettler Toledo STARE system in the tension mode (Mettler Toledo, Switzerland). The elastic modulus *E'* and the loss factor (*tan δ*) were measured in a frequency of 0.1-10Hz and both values were determined as a function of frequency.

### 3.5. Conductivity Measurements

The dielectric parameters of the nanocomposites were analyzed using an Ando AG-4311 LCR meter (USA) in low frequencies from 100 Hz to 100 KHz. Frequencies from 100 KHz to 120 MHz were applied from a Hioki LCR 3535-Hi Tester meter (Hioki Co., Japan). The experiments were carried out using a 9699 SMD test fixture with electrodes fitted with sample object sizes of 1.0 mm width 4.0 mm length and less than 1.5 mm height. The test fixture was set at an operating frequency range from 0.1Hz to 120 MHz. The voltage was varied from -0.01 to 0.01V in steps of 0.001V at 1sec intervals.

## 4. Results and Discussions

### 4.1. Scanning Electron Microscopy and Energy Dispersive Spectroscopy Analysis of Nanocomposites

Scanning Electron Microscopy and Energy Dispersion Spectroscopy were used to study the dispersion of the nanofibres in the polymer. The SEM images of the nanocomposite showed the matrix with the domain size of nanoparticles while the carbon nanofibers had a smaller percentage but of higher size, the cross-section images showed fibers that were well spread and embedded into the matrix, this showed that the nanocomposite had been formed. The image (Figure 1, 0.2%

nanocomposite) shows a homogeneous and fine dispersion of nanofibers in the matrix with interconnections that demonstrate better compatibility between the fiber and matrix and ensure improved mechanical strength of the nanocomposite

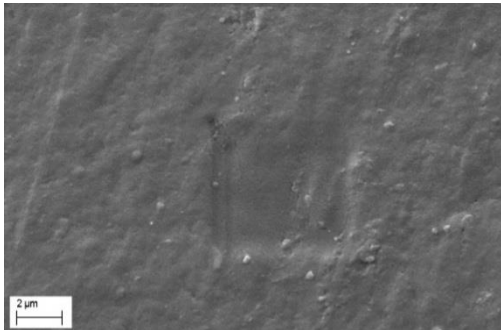


**Figure 1.** Cross-section Scanning Electron micrograph of 0.2% Butyl carbon nanocomposites.

Fractured nanocomposite **Figure 2** that had a single fibre pull out was also studied to ascertain the distribution of the fibers in the matrix and the impediment of the fibre into the cellulose matrix.



**Figure 2.** SEM image of a fractured nanocomposite single fiber pull-out.

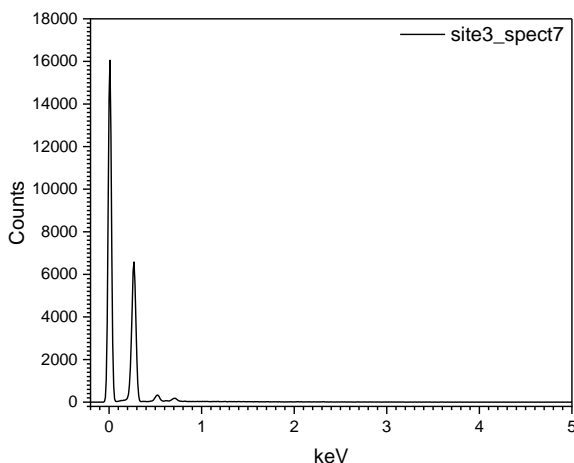


**Figure 3.** Energy dispersion images of nanocomposite derived from acetyl-nanofiber.

The Energy Dispersion spectrum of Acetyl-derived nanocomposite showed a single peak of carbon and a trace of oxygen in the nanocomposite (**Figure 3**), confirming the composition of the nanocomposite.

## 4.2. Thermal Analysis of Nanocomposites

The mass degradation temperature is a crucial factor that determines how well nanocomposites function in high-temperature settings. Thermal Gravimetric Analysis as a function of weight loss against the temperature for the blank sample is presented in **Figure 4**. The TGA curve shows a gradual decrease in weight as the temperature increases up to 300 °C, this initial part represents the sample burning leading to loss of moisture or residue organic solvents and most probably emission of some gases. The sample then sharply lost weight starting at 330 °C, followed by further weight loss degradation from 400 °C to 600 °C, where the curve leveled out representing the residue fractions of graphitic carbon [14]. It is worth noting that the significant loss of weight recorded at approximately 330 °C and 400 °C, as seen on the TGA curve coincides with the degradation peak of the derivative and could be due to the breakdown of the backbone of the polymer ascribed to the decomposition of the material. The aggregate weight loss was approximately 70%. [15].

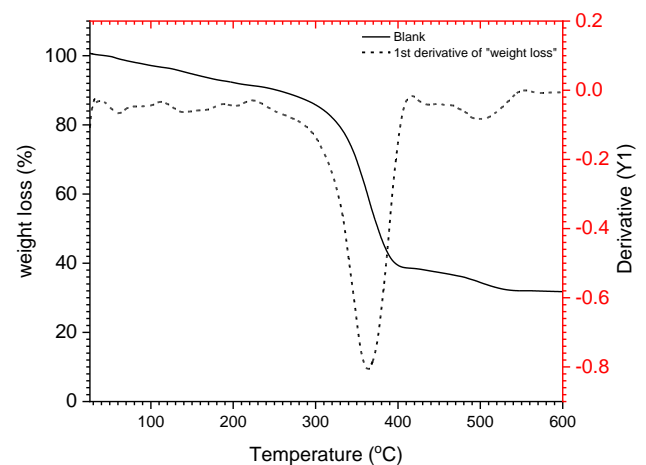


**Figure 4.** TGA and dTGA of the blank-reference sample.

The nanocomposites of functionalized 0.2 Acetyl, 0.2 Butyl, and 0.2 Acetyl were also tested for thermal stability. The TGA and dTG of the nanocomposites exhibited the same trend as the blank sample with an initial decrease in weight before a sharp loss at approximately 350 °C, the derivative peak also coincides with one of the blank sample, however, the degradation was more at 80%, 84%, 80%, respectively compared to the blank. The 0.4 Butyl, 0.4 Dodecyl, and 0.4 Acetyl carbon nanocomposite, registered degradation, and decomposition levels of approximately 92%, 84%, and 90%, respectively. The observed characteristics suggest that the surface modifi-

cations culminated in an increased thermal stability of the native cellulose-nanocomposite, compared to the blank material. This observation is in harmony with other common modifications, which significantly increased the degradation temperature of cellulose as reported in the literature [15]. The increase could be attributed to the formation of networks of polymer chains and the nanofibres which could then restrict the movement of the free atoms. The TGA analysis of cellulose triacetate also revealed an increase in glass transitional temperature  $T_g$  from the expected value of  $153^\circ\text{C}$  to a higher  $T_g$  of  $350^\circ\text{C}$  that could be attributed to the use of Cetyltrimethylammonium bromide as a plasticizer. The blank sample decomposed to 80% less its weight at  $380^\circ\text{C}$  leaving 20% of the polymer as a residue (Figure 5).

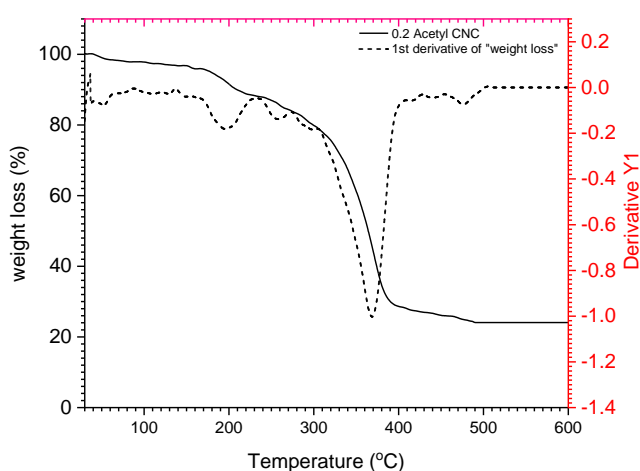


Figure 5. TGA and dTGA of blank matrix and nanocomposites.

### 4.3. Dynamic Mechanical Analysis of Nanocomposites

Mechanical analysis of nanocomposites of 0.2% n-butyl, acetyl, and dodecyl functionalized carbon nanofibres in cellulose acetate polymers revealed that their storage modulus was not initially affected at lower temperatures of  $27\text{--}37^\circ\text{C}$  but starts to reduce as the temperature increases up to  $180^\circ\text{C}$  where they flatten out, (Table 1; Figure 6).

Table 1. Storage modulus (MPa) of functionalized carbon nanofibres nanocomposites.

Sample	0.2%		0.4%	
Temp	$37^\circ\text{C}$	$180^\circ\text{C}$	$37^\circ\text{C}$	$180^\circ\text{C}$
Acetyl	990	220	460	210
Butyl	1690	220	1801	210
Dodecyl	1750	220	2250	220
Reference	1400	220	1400	220

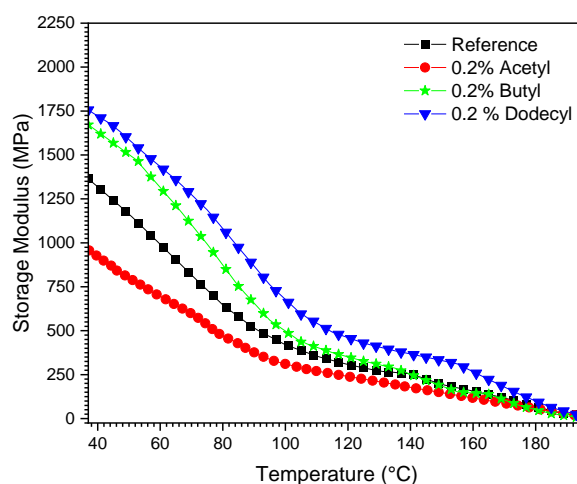


Figure 6. Storage modulus of nanocomposite from 0.2% f- carbon nanofiber.

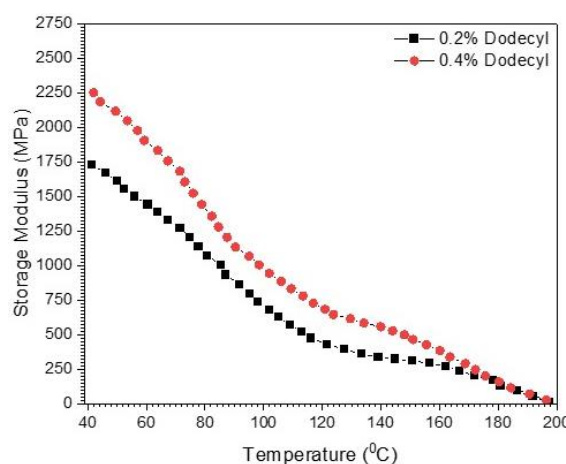


Figure 7. Comparison of storage modulus of 0.2% and 0.4% nanocomposites.

It was observed that functionalization increases the stiffness of nanocomposites, except in the case of acetyl, which results in a brittle nanocomposite. The increase in stiffness can be explained by the ability of small, functionalized carbon nanofibres to fill spaces within the polymer matrix with stronger interfacial interactions, resulting in increased adherence between the nanoparticles and polymer matrix, the nanofibres are thought to have immobilized the polymer matrix chains leading to the rigidity [14]. Reduced storage modulus at increased temperature is associated with an increase in the kinetic energies of nanofibres leading to a decrease in stiffness [16]. Also, functionalization with butyl resulted in the highest storage modulus, while acetyl had the lowest. This can be attributed to differences in interactions between the functionalized nanofiber and the polymer matrix. Comparing the storage modulus of the nanocomposites also revealed a marginal increase as the filler increased from 0.2% to 0.4% [17] as shown in Figure 7. This could be attributed to the stiffening of the polymer matrix as the more nanofibres

filled the voids or spaces/moieties between the polymer chains and increased the rigidity of the sample.

The measurement of the glass transition temperature of the

blank and nanocomposites revealed an increase upon the addition of functionalized nanofibers to the polymer (Table 2).

**Table 2.** Glass transitional temperature  $T_g$  and  $Tan\ Delta$  values of 0.2% and 0.4% nanocomposites.

Sample	0.2%		0.4%	
	Tg °C	Tan Delta ( $\delta$ )	Tg °C	Tan Delta ( $\delta$ )
Acetyl	196 $\pm$ 2	0.58	199 $\pm$ 1	0.49
Butyl	196 $\pm$ 2	0.49	200 $\pm$ 1	0.46
Dodecyl	172 $\pm$ 2	0.62	182 $\pm$ 1	0.38
Reference	160 $\pm$ 1.5	0.67	160 $\pm$ 1.5	0.67

Compared to the reference sample, whose transition temperature is 160 °C, that of nanocomposites with 0.2% acetyl and butyl functionalized nanofiber filler was 196  $\pm$  2 °C, while that of dodecyl was 172  $\pm$  2 °C. This shows a general increase in glass transition temperature upon the addition of functionalized carbon nanofiber. A plot of loss factor ( $\tan \delta$ ) vs temperature of 0.2% acetyl, butyl, and dodecyl containing nanocomposites compared to a blank reveals a steady increase after 100 °C to a maximum value estimated as the glass transition temperature of the reference and nanocomposites. This is illustrated in Figure 8 below.

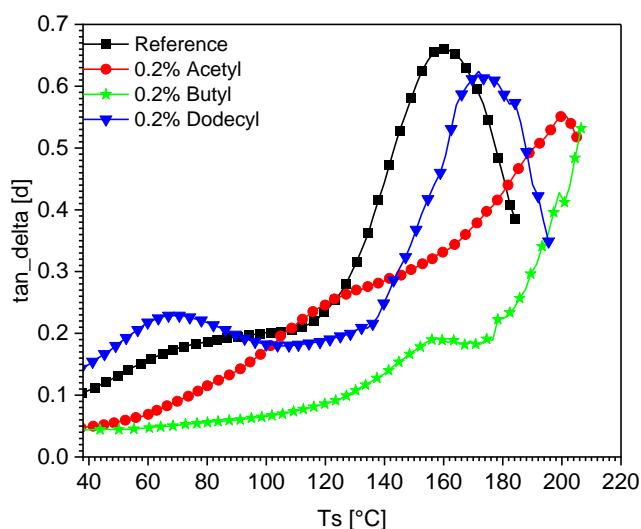


**Figure 8.** Tan delta plots of nanocomposites of 0.2% f-carbon nanofiber.

Increasing the carbon nanofiber composition from 0.2 wt% to 0.4 wt% of the nanocomposite resulted in a reduction of  $\delta$  from 0.67 of the reference sample to 0.5, as shown in Figure 9 below. The values above show that the addition of the nano-

fibers reduces the mobility of the cellulose molecules due to the interfacial interaction of the nanofibers and the polymer, leading to stiffening of the polymer and a low viscosity of the resulting nanocomposite. The assumption is that there is an increase in interfacial interaction linked to the large specific surface area of the functionalized carbon nanofibers and their higher thermal stability that reduces the mobility leading to an increase in the  $T_g$  of the samples [18].

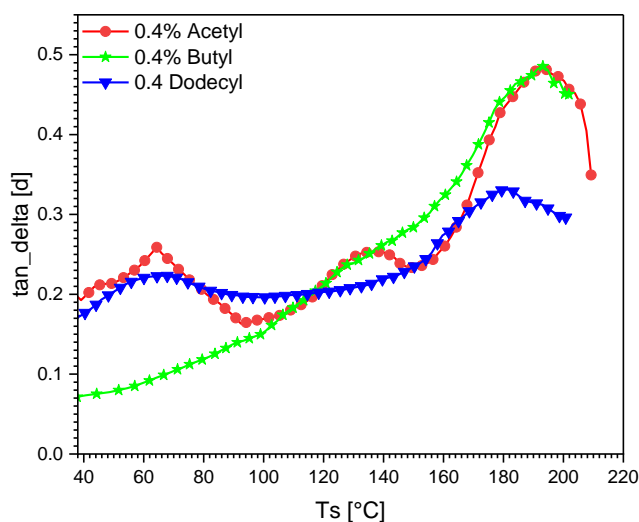


**Figure 9.** Tan delta plots of 0.2% nanocomposites.

Further comparison of  $T_g$  and  $\delta$  values of 0.2% and 0.4% concentrations of CNF further revealed an important relationship between CNF concentration and viscosity. For instance, Dodecyl plots (Figure 10) show that the 0.2%  $T_g$  is at a lower temperature (172 °C) with a higher value of  $\tan \delta$  (0.62) compared to the 0.4% transitional temperature (182 °C) and a lower  $\tan \delta$  (0.38) indicating that an increase in the percentage of nanofiber in the matrix leads to a decrease in the viscosity

of the nanocomposite or the increase in mechanical strength of the nanocomposite.

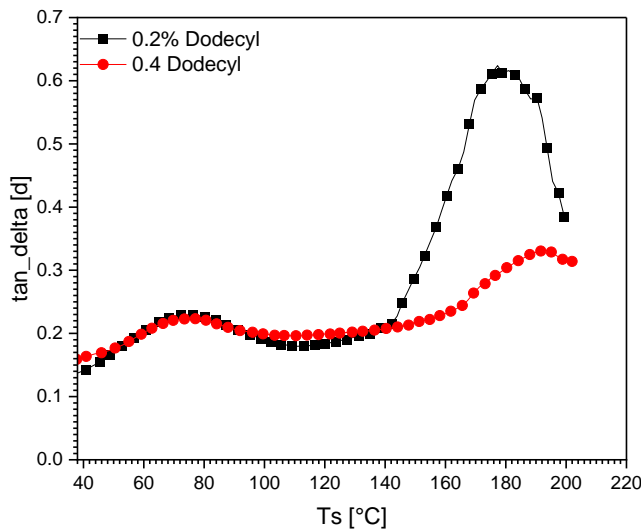


**Figure 10.** Comparison of tan delta of 0.2% and 0.4% of the dodecyl nanocomposite.

#### 4.4. Conductivity and Permittivity of Nanocomposites

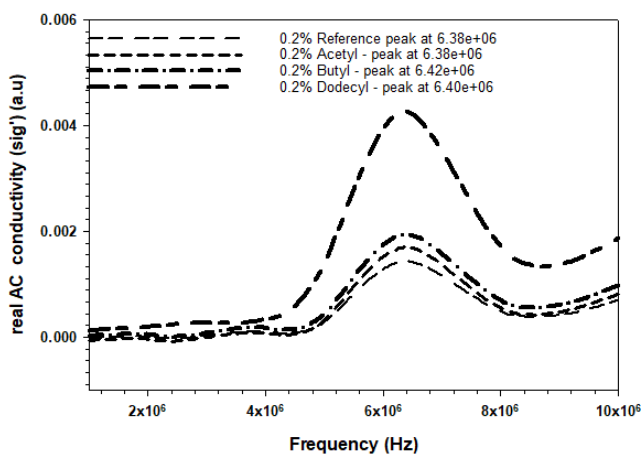


**Figure 11.** Conductivity measurements of the 0.2% nanocomposites and the reference.

Conductivity and permittivity tests of 0.2% and 0.4% nanocomposites, as well as the reference/blank (cellulose acetate, the dispersant, and the plasticizer), were done at room temperature as a function of frequency in the range 10<sup>2</sup>-10<sup>8</sup> Hz. The electrical conductivity for 0.2% nanocomposites of dodecyl, butyl, and acetyl is shown in Figure 11. As the frequency increases from 1x10<sup>2</sup> to 4 x 10<sup>5</sup> Hz, the conductivity remains similar for all the samples, irrespective of the CNF concentrations in the nanocomposite, including the reference material, but towards 6 x 10<sup>5</sup> Hz, the conductivity increases,

with dodecyl having the highest change and black having the least change; they all peak off at mid-6 x 10<sup>6</sup> to 7 x 10<sup>6</sup> Hz and then decrease.

Generally, the interfacial polarization is critical in determining the dielectric properties of the nanocomposites at low frequencies. The interfacial polarization is strong, but as the frequency increases, it gradually weakens due to the increased oscillation of the applied electric field, leading to a decrease in the dielectric constant and a surge in conductivity. [21, 22].

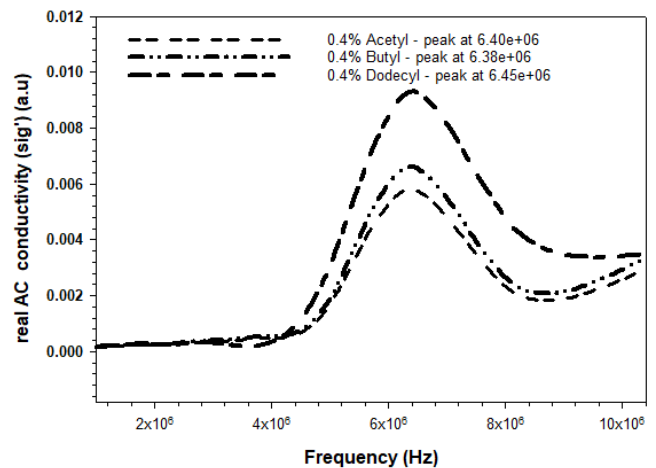


**Figure 12.** Conductivity measurements of the 0.4% nanocomposites.

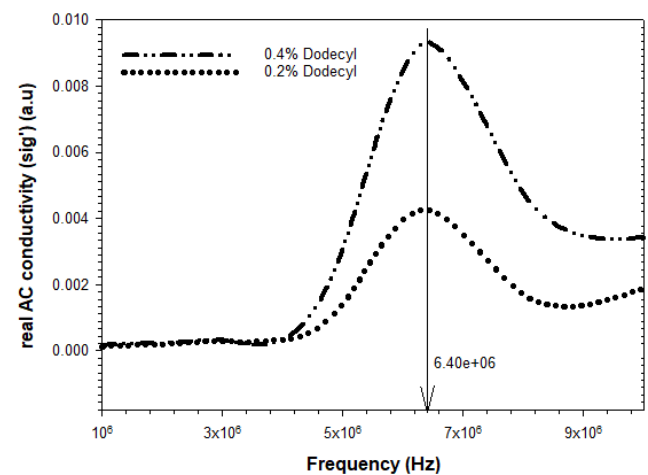


**Figure 13.** Comparison of Conductivity measurements of 0.2% and 0.4% dodecyl nanocomposites.

This could be attributed to the large volume fraction of interfaces of the nanocomposites that makes them more susceptible at high frequencies, which then decline beyond a given frequency. The reference material has a higher dielectric value than the 0.2% nanocomposites, meaning that the addition of the CNF led to a decrease in the dielectric constant of the nanocomposites. This is affirmed in the 0.4% nanocomposites Figure 12, which shows a further decrease in the dielectric constant of the nanocomposite with the increase in

nanofiber composition in the nanocomposite.

The dodecyl functionalized fibers had more effect than butyl and acetyl. A comparison of 0.2% and 0.4% dodecyl is shown in Figure 13, where the conductivity of the 0.4% dodecyl has a higher peak value compared to the 0.2% dodecyl nanocomposite. As earlier stated, the increases in conductivity or decrease in dielectric constant are due to the good electrical conductivity and dispersion of the CNF in the nanocomposite. It is important to note that the 0.4% composition of the nanocomposite does not yet transit the polymer from insulator to semiconductor, at least 2% of CNF is needed to transit the polymer [22].

## 5. Conclusions

The study demonstrates the successful addition of functionalized carbon nanofibers to the cellulose acetate matrix and the effect of this on the mechanical, thermal, and electrical properties of the resulting nanocomposites. Cross-section SEM and EDS are used to confirm the embedment of CNFs into the cellulose acetate matrix. The decomposition patterns of the resulting nanocomposites compared to the reference standard reveal an increase in the thermal strength of nanocomposites containing CNF. Increased stiffness upon the addition of CNF to the matrix compared to the reference was also observed, accompanied by a reduction in storage modulus. The glass transition temperature, viscosity, and conductivity of the nanocomposites marginally increased upon the addition of functionalized CNF to the matrix. It was further established that when wt% of CNF in the polymer matrix is increased by 50% (0.2- 0.4 wt%), the mechanical and electrical properties of the nanocomposites formed also change with an increase in the storage modulus/strength of the nanocomposite and improved electrical properties. The unique properties of the nanocomposites can be applied in the production of new nanomaterials of varied industrial applications.

## 6. Recommendations

To further enhance the knowledge of properties and applications of CNF-based nanocomposites, future research should explore a wider range of functional groups beyond alkylation, including amine, and investigate the effects of tailoring these groups. Since a biodegradable polymer matrix has been used, further studies should be carried out on the durability of the nanocomposites in the environment to help inform their applications.

## Abbreviations

CA	Cellulose Acetate
CNF	Carbon Nanofibers
DMA	Dynamic Mechanical Analysis

DTA	Differential Thermal Analysis
EDS	Energy Dispersive Spectroscopy
FTIR	Fourier Transform Infra-Red
PTFE	Polytetrafluoroethylene
PMMA	Poly (Methylmethacrylate)
SEM	Scanning Electron Microscopy
T <sub>g</sub>	Glass Transition Temperature
TGA	Thermal Gravimetric Analysis

## Acknowledgments

The authors gratefully acknowledge the National Research Fund -Kenya for partially funding this work. We also express our sincere appreciation to the International Atomic Energy Agency- Seibersdorf laboratories, and the staff at the School of Chemistry and Material Science, The Technical University of Kenya, for their invaluable contributions.

## Conflicts of Interest

The authors declare no conflict of interest.

## References

- [1] Satish K., Hant D., Mohan S., Jung O., David S. (2002). Fibers from Polypropylene/nano carbon fiber nanocomposite. *Polymer Communication*, 43, 1701-1703. [https://doi.org/10.1016/S0032-3861\(01\)00744-3](https://doi.org/10.1016/S0032-3861(01)00744-3)
- [2] Nitilaksha H., Sunay B., Ramiz B., Maria C., Amit K., Jimmy M., Gajanan B. (2023). Carbon nanofibers-based carbon-carbon nanocomposite fibers. *Discover Nano*, 18: 159. <https://doi.org/10.1186/s11671-023-03944-z>
- [3] Alejandro J., Rodriguez M., Guzman C., Bob M. (2010). Mechanical properties of carbon nanofiber/fiber-reinforced hierarchical polymer nanocomposites manufactured with multiscale-reinforcement fabrics. *CARBON*, 49: 937–948. <https://doi.org/10.1016/j.carbon.2010.10.057>
- [4] Joshi M., Bhattacharyya A. (2004). Carbon Nanofiber Reinforced Carbon/Polymer Nanocomposite. *NSTI-Nanotech 3*: 134-138. [www.nsti.org](http://www.nsti.org), ISBN 0-9728422-9-2
- [5] Dafeng Yan, Shuo Dou, Li Tao, Zhijuan Liu, Zhigang Liu, Jia Huo and Shuangyin Wang 2016: Electropolymerized supermolecule derived N, P co-doped carbon nanofiber networks as a highly efficient metal-free electrocatalyst for the hydrogen evolution reaction; *J. Mater. Chem. A*, 4, 13726-13730. <https://doi.org/10.1039/C6TA05863A>
- [6] Minghuan Liu, Xiao-Peng Duan, Ye-Ming Li, Da-Peng Yang, Yun-Ze Long 2017, Electrospun nanofibers for wound healing, <https://doi.org/10.1016/j.msec.2017.03.034>
- [7] Ana M. Martins, George Eng, Sofia G. Caridade, et al, 2014: Electrically Conductive Chitosan/Carbon Scaffolds for Cardiac Tissue Engineering *Biomacromolecules*, 15, 635–643 <https://doi.org/10.1021/bm401679q>

- [8] Kumari, S., Mishra, R.K., Parveen, S. et al. 2024 Fabrication, structural, and enhanced mechanical behavior of MgO substituted PMMA nanocomposites for dental applications. *Sci Rep* 14, 2128. <https://doi.org/10.1038/s41598-024-52202-4>
- [9] Min-Ho Kang, Tae-Sik Jang, Hyun-Do Jung, Sae-Mi Kim, Hyoun-Ee Kim, Young-Hag Koh, Juha Song (2016) Poly (ether imide)-silica hybrid coatings for tunable corrosion behavior and improved biocompatibility of magnesium implants *Biomed. Mater.* 11 035003  
<https://doi.org/10.1088/1748-6041/11/3/035003>
- [10] Nakamura, M.; Ueda, K.; Yamamoto, Y.; Aoki, K.; Zhang, M.; Saito, N.; Yudasaka, M. (2022) Bisphosphonate type-dependent cell viability suppressive effects of carbon nano horn-calcium phosphate-bisphosphonate nanocomposites. *Biomater. Sci.* 10, 6037–6048.  
<https://doi.org/10.1039/d2bm00822j>
- [11] Yu Chen et al., "Investigation on Space Environmental Degradation Effects of Solar Cell Coverglass," in *IEEE Transactions on Plasma Science*, vol. 41, no. 12, pp. 3471-3476, Dec. 2013, <https://doi.org/10.1109/TPS.2013.2280287>
- [12] Ayesha K., Patrizia B. (2022). Poly (methyl methacrylate) Nanocomposite Foams Reinforced with Carbon and Inorganic Nanoparticles—State-of-the-Art. *J. Compos. Sci.* 6, 129.  
<https://doi.org/10.3390/jcs6050129>
- [13] Liang, F., Sadana, A. K., Peera, A., Chattopadhyay, J., Gu, Z., Hauge, R. H., & Billups, W. E. (2004). A Convenient Route to Functionalized Carbon Nanotubes. *Nano Letters*, 4(7), 1257–1260. <https://doi.org/10.1021/nl049428c>
- [14] Wang H, Xu P, Zhong W, Shen L, Du Q. (2005) Transparent poly (methyl methacrylate)/silica/zirconia nanocomposites with excellent thermal stabilities. *Polymer Degradation and Stability* 2005; 87: 319-27.  
<https://doi.org/10.1016/j.polymdegradstab.2004.08.015>
- [15] Elsayed Elbayoumy, Nasser A. El-Ghamaz, Farid Sh. Mohamed, Mostafa A. Diab, Tamaki Nakano, (2021) Dielectric Permittivity, AC Electrical Conductivity and Conduction Mechanism of High Crosslinked-Vinyl Polymers and Their Pd (OAc)<sub>2</sub> Nanocomposites *Polymers*, 13, 3005  
<https://doi.org/10.3390/polym13173005>
- [16] Sampat Chauhan, Bhanu Pratap Singh, Rajender Singh Malik et al et al (2018) Detailed Dynamic Mechanical Analysis of Thermomechanically Stable Melt-Processed PEK–MWCNT Nanocomposites, *Polymer Nanocomposites—2018*.  
<https://doi.org/10.1002/pc.24247>
- [17] Tshwafo Elias Motaung, Adriaan Stephanus Luyt, Federica Bondioli et al, 2012 PMMA-titania nanocomposites: Properties and thermal degradation behaviour, *Polymer Degradation and Stability* 97, 1325-1333  
<https://doi.org/10.1016/j.polymdegradstab.2012.05.022>
- [18] Neira-Velázquez M., Guadalupe R., Valle L., Hernández-Hernández E., Zapata-González I. (2008). Surface modification of carbon nanofibers (CNFs) by plasma polymerization of methylmethacrylate and its effect on the properties of PMMA/CNF nanocomposites. *Polymers*. 162, 1-11.  
<https://doi.org/10.1515/epoly.2008.8.1.1855>
- [19] Xianglong Li; Jiahua Shi; Yujun Qin; Qi Wang; Hongxia Luo; Pu Zhang; Zhi-Xin Guo; Hyung-Suk Woo; Dong-Kyu Park. (2007). Alkylation and arylation of single-walled carbon nanotubes by mechanochemical method. *Chemical Physics Letters*. 444(4-6), 258-262.  
<https://doi.org/10.1016/j.cplett.2007.07.016>
- [20] Lichao Feng., NingXie., Jing Z. (2020). Carbon Nanofibers and Their Nanocomposites: A Review of Synthesizing, Properties and Applications. *Materials*, 7, 3919-3945.  
<https://doi.org/10.3390/ma7053919>
- [21] Ling Zhang Ling Zhang. (2020). Applications, Challenges, and Development of Nanomaterials and Nanotechnology. *Journal of the Chemical Society of Pakistan*, 42(5).  
<https://doi.org/10.52568/000690/JCSP/42.05.2020>
- [22] Diab, M. A.; El-Ghamaz, N. A.; Mohamed, F. S.; El-Bayoumy, E. M. (2017) Conducting polymers VIII: Optical and electrical conductivity of poly (bis-m-phenylenediaminosulphoxide). *Polym. Test.*, 63, 440–447.  
<https://doi.org/10.1016/j.polymertesting.2017.09.001>